

Examination of Barkhausen noise parameters for characterisation of strain-induced martensitic transformation in AISI 304 stainless steel

E Ahmadzade-Beiraki, M Mazinani and M Kashefi

In this study, the strain-induced martensitic transformation in AISI 304 stainless steel after tensile deformation was investigated using different magnetic Barkhausen noise (MBN) parameters. For this purpose, different amounts of martensite phase were formed in AISI 304 stainless steel by different amounts of tensile deformation. The amount of strain-induced martensite phase in the steel samples was quantified by XRD patterns. The MBN profile and the RMS voltage of the MBN parameters were employed in order to evaluate the microstructural changes. The MBN parameters (RMS and peak height) increased with the amount of deformation and this was attributed to the volume fraction of magnetic domains and pinning sites increasing with the increase in martensite content. It was suggested that the growth of martensite laths provided wider areas for the motion of domain walls and their interaction with obstacles within the martensite, resulting in an increasing rate of change in the RMS values and the width of the MBN profile with martensite content. However, the coalescence of martensite packets decreased the number of Barkhausen signals being emitted from the austenite-martensite interface areas, resulting in a decrease in the slope of the peak height curve with increasing martensite content.

Keywords: magnetic Barkhausen noise, non-destructive evaluation, strain-induced martensite, austenitic stainless steel.

Introduction

Austenitic stainless steels have superior corrosion resistance, formability and weldability among all the stainless steel alloys. This class of stainless steels has a wide range of engineering applications, including in the petrochemical and power industries^[1]. These highly-alloyed stainless steels are relatively stable and transform into martensite only by quenching to sub-zero temperatures, although the low-alloyed grades, known as metastable austenitic stainless steel, transform into martensite by both quenching to sub-zero temperatures and by cold working at room temperature. This type of martensitic transformation during deformation of metastable austenite is called deformation-induced martensitic transformation. There are two types of deformation-induced martensite phase, *ie* ϵ -martensite with an hcp crystal structure as well as α' -martensite with a bcc crystal structure. The α' -martensite phase can be produced from the austenite phase and/or directly from the ϵ -martensite phase during deformation^[2].

The non-destructive Barkhausen noise (BN) test technique is widely used for the microstructural characterisation of ferromagnetic materials^[3-27]. This method is mostly based on the irreversible domain wall (DW) motions from pinning sites^[3]. Lattice imperfections, such as grain boundaries, dislocations and precipitates, obstruct the motion of domain walls until an increase in the applied magnetic field (H) provides the energy necessary to free the pinned domain walls from obstacles. This un-pinning phenomenon occurs by a sudden jump producing a magnetic flux change called Barkhausen noise. Other sources of BN are nucleation and annihilation of the magnetic domains at phase or grain boundaries during magnetisation^[3-6]. The BN signal provides various parameters, including peak height, peak position and the width of the BN profile, RMS value, frequency amplitude spectrum and pulse height distribution^[7], which, in particular cases, may be used individually as a parameter representing a given feature

of the material microstructure. As relevant examples indicating the appropriateness of these parameters in the characterisation of engineering materials, peak and RMS values decrease with an increase in the grain size^[8-12], a decrease in the pearlite content in both hypo- and hypereutectoid steels^[13], an increase in the martensite content in dual-phase steels^[14] and a decrease in the martensite volume fraction in austenitic stainless steels^[15,16]. The peak position (PP) of a BN profile represents the magnetic coercivity (H_c) indirectly^[17-19], which has been used for the evaluation of microstructural changes in different steels^[20-22]. The width of a BN profile shows, more appropriately, the trend through which the hardness of ground steels are represented^[23]. The pulse height distribution has been used for determination of the carbon content of steels^[24] and the extent to which a steel is tempered^[25]. The BN frequency spectrum has also been employed in order to evaluate the variation of grain size effects^[9] and tempering processes^[26].

The main aim of the present study has been to investigate the novel applicability of MBN parameters to the process of strain-induced martensitic transformation in an austenitic stainless steel. The important difference between this study and the previous studies on the magnetic Barkhausen noise characterisation of strain-induced martensite^[14,15] is that, in the present study, an attempt has been made to explain how the amount and size of α' -martensite affect the MBN parameters of RMS and peak height.

● Submitted 18.12.15 / Accepted 25.04.16

Esmael Ahmadzade-Beiraki, Mohammad Mazinani and Mehrdad Kashefi are with the Department of Materials Engineering, Faculty of Engineering, Ferdowsi University of Mashhad, PO Box 91775-1111, Mashhad, Iran.*

**Corresponding author. Tel/Fax: +98 5138763305; Email: m-kashefi@um.ac.ir*

Experiment

Eight tensile samples were prepared according to the ASTM-E8M standard test procedure from a 2 mm-thick sheet of AISI 304 stainless steel with the chemical composition given in Table 1. All test samples were first solution-treated at 1095°C for 1 h and then water quenched to room temperature in order to prevent any carbide precipitation during cooling. To produce different amounts of martensite, the test samples were deformed to 0.05, 0.1, 0.15, 0.25, 0.3, 0.35, 0.4 and 0.44 true strain values using a Zwick/Z250 tensile testing machine with an average strain rate of 0.002 s⁻¹ at room temperature. Vickers hardness measurements were carried out on the samples at 30 kg and room temperature.

Table 1. Chemical composition of the investigated stainless steel

Element	Cu	Ni	Mn	Cr	Si	P	C	Fe
[wt%]	0.428	8.719	1.350	16.785	0.598	0.041	0.056	Bal

Optical microscopical examinations were carried out on test samples after being prepared by conventional metallographic preparation methods. All samples were electro-polished for 40 s at 18 V in an electrolyte bath consisting of 110 ml perchloric acid, 180 ml ethanol and 710 ml methanol. The Beraha's reagent (0.5 g potassium metabisulfite, 20 ml HCl and 100 ml distilled water) was used to reveal the martensite phase in the steel microstructures and a solution of 60% HNO₃ in 40% distilled water was employed for etching the grain boundary areas. XRD measurements were carried out using a Philips X'pert diffractometer with Cu-K α radiation. The volume fraction of α' -martensite was measured from the XRD patterns according to the ASTM E975-03 standard test procedure. The volume fraction of α' -martensite of the samples are presented in Table 2.

Table 2. Martensite percentage of tensile-strained samples

True strain	0	0.05	0.1	0.15	0.25	0.3	0.35	0.40	0.44
α' -martensite%	3	9	20	24	41	48	58	66	80

The experimental set-up developed for the MBN measurements is illustrated in Figure 1. A multi-frequency function generator was used to supply a sinusoidal current (4 Hz) to the excitation coil of a yoke with 3000 turns, which generates a magnetisation force to be applied to the test sample through the U-core poles. Barkhausen signals during magnetisation were picked up by means of a surrounding coil with 3000 turns. The pick-up voltage was filtered (0.2 kHz high-pass filter), amplified and, finally, converted to digital data to be used as readable input for a personal computer. Barkhausen signals in three magnetisation cycles were processed

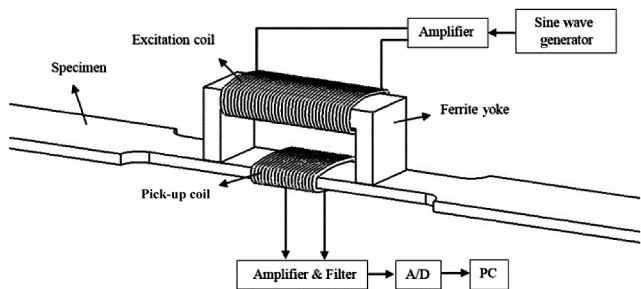


Figure 1. Schematic of the experimental set-up used for Barkhausen noise measurements

for each test sample and the parameters of RMS voltage and BN profile were obtained by averaging from these three cycles and employed in order to characterise the microstructural changes in the test samples during deformation.

Results and discussion

Results of optical microscopy and hardness measurement

Figure 2 exhibits the microstructures of undeformed (solution-treated) and deformed (for the tensile true strains of 0.05, 0.25 and 0.44) samples. The microstructure of the undeformed sample consists of equiaxed austenite grains with an average size of 46 μ m along with the annealing twins within the austenite grains. Dark areas in the microstructures are strain-induced martensite that has been formed during deformation (around 9%, 41% and 80% for the true strains of 0.05, 0.25 and 0.44, respectively).

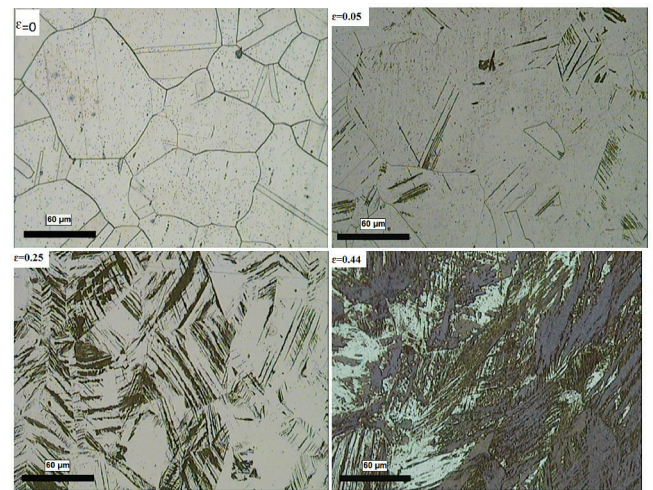


Figure 2. The microstructure of the solution-treated sample ($\epsilon = 0$) and the deformed samples to the true strains of 0.05, 0.25 and 0.44. The martensite content in the deformed samples is 9%, 41% and 80%, respectively

The variation of the Vickers hardness of samples with martensite percentage is shown in Figure 3. As can be seen, the hardness increases almost linearly with martensite content.

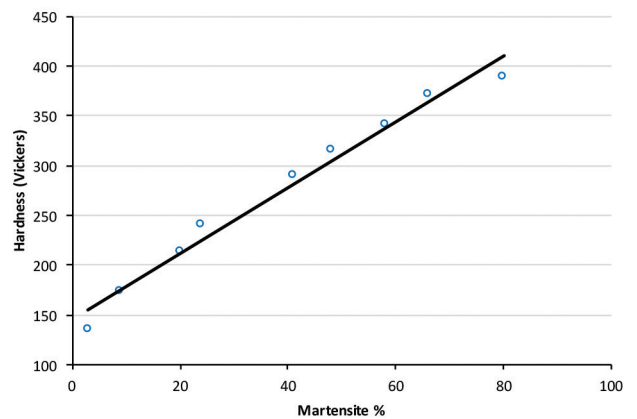


Figure 3. The variation of Vickers hardness with martensite percentage

Barkhausen noise characterisation

The BN profiles of test samples with true strains of 0.25 to 0.44 are shown in Figure 4. The BN profile represents the Barkhausen noise shape and reflects information about the material properties. The peak height parameter is the maximum point of this dome-shaped curve (BN profile). For the samples with lower strain values, the density of Barkhausen signals has not been high enough in order for the BN profile to be plotted with the same parameters used for higher strain values.

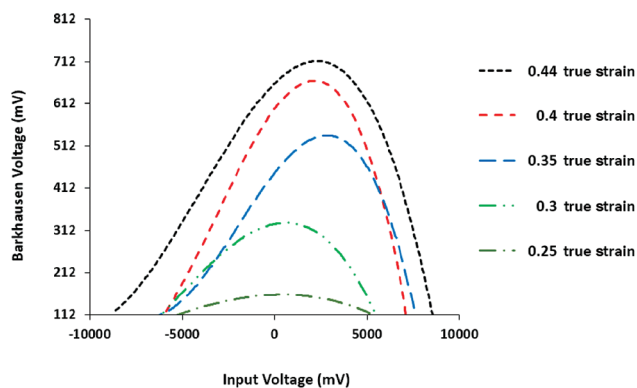


Figure 4. BN profiles of the test samples with true strains of 0.25 to 0.44

Variations of the RMS, peak height and full width at half maximum (FWHM) with martensite content in steel microstructures are illustrated in Figure 5. It can be observed that all three parameters increase with the percentage of martensite. In fact, the interaction of DWs with pinning points such as dislocations, twins or lath boundaries^[15] generates Barkhausen signals that depend on the volume fraction of DWs as well as the pinning sites. Thus, the mentioned increase in MBN parameters can be attributed to an increase in the volume fractions of magnetic domains and pinning sites, which increase, in turn, with the increasing martensite content.

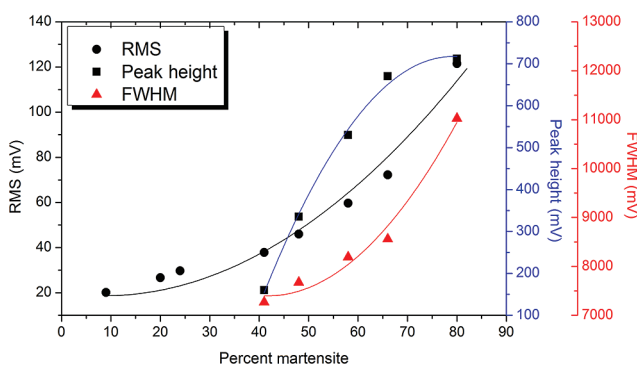


Figure 5. Variation of the MBN output, including RMS, peak height and FWHM with martensite content

Another significant change in MBN parameters with martensite content is in the slopes of corresponding curves. The slopes of RMS and FWHM increase progressively with the percentage of martensite, whereas the peak height increases continuously with a decreasing slope. In the same way as with the microstructure of the sample with 0.05 true strain in Figure 2, when the volume fraction of α' -martensite is relatively low, thin martensite laths are randomly distributed in the austenitic matrix. The distances

between the ferromagnetic phases are high in this situation. Hence, the interaction of DWs with microstructural obstacles are limited in these isolated ferromagnets (α' -martensite). As can be seen in the microstructure of the sample with 0.44 true strain in Figure 2, further deformation results in larger martensite packets, which provides more extensive areas for DW motion. In an extensive ferromagnetic phase, DWs interact with more obstacles and generate more Barkhausen signals up to the saturation point^[27]. To have a better understanding of how the morphology of the martensite phase affects the MBN, the variation of the pinning strength of obstacles is illustrated in Figure 6, in which the DW interaction with obstacles is plotted for the cases when martensite islands are thin (Figure 6(a)) and when they are relatively wide (Figure 6(b)). The experimental results in the literature with regard to the influence of interfaces such as grain or inter-phase boundaries on the formation of MBN^[8,9,12,13,28,29] indicate that the austenite-martensite interface can be considered to be a strong pinning site. It has been suggested that the grain boundaries act as highly dense small pinning sites and the sudden release of DWs from this type of pinning site generates a large peak in the BN profile^[12]. The pinning effect of cementite-ferrite interfaces has also been considered to be the main reason for the variation of MBN with the carbon content of steel^[12]. A reduction of the magnetic coercivity of austenitic stainless steels with an increase in the martensite content (as a result of the austenite to martensite transformation by deformation) has also been suggested to be due to a decrease in the austenite-martensite interface, which can act as a strong pinning site^[29]. It can then be concluded that other obstacles within the martensite phase (mostly dislocations) represent lower pinning strengths than those generated by the austenite-martensite interface. As shown in Figure 6, the DWs obstructed by austenite-martensite interfaces need higher levels of applied magnetic forces than those needed by other obstacles. As a result, during the stage of releasing the DWs from the austenite-martensite interfaces, they will have enough energy to pass the subsequent low-energy obstacles without being pinned by them. In the low deformation regime where the martensite phase is very thin (as for the sample with 0.05 true strain in Figure 2), the magnetic domains are restricted by the lath boundaries and tend to be stretched between them. Upon application of the magnetic field, the magnetic domains grow and quickly reach the lath boundaries, after which the DWs can only move in a direction parallel to the martensite lath. In this situation, where the DWs are continuously in touch with the lath boundaries, a situation similar to that shown in Figure 6(a) occurs. Consequently, at the beginning stages of deformation, the formation of Barkhausen noise is mostly due to the fact that the DWs pass through the austenite-martensite interfaces. As the deformation increases, the martensite packets grow (as for the sample with 0.44 true strain in Figure 2) and DWs

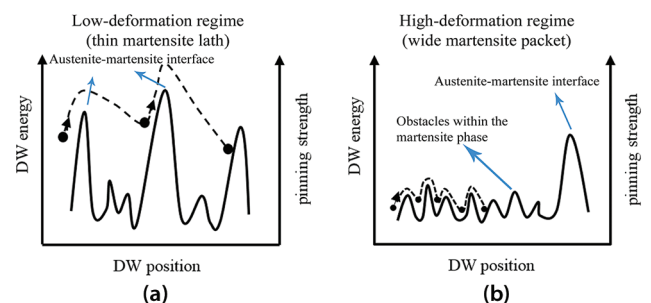


Figure 6. Representation of DWs' interaction with obstacles in low- and high-deformation regime

with no connection with the lath boundaries can interact with the obstacles within the martensite phase and thus the Barkhausen signals will be generated (Figure 6(b)). The signals emitted from inside the martensite phase are within the wide range of applied magnetic fields, which are related to a variety of obstacles within the martensite having various pinning capabilities. Therefore, one may conclude that the increasing rate in the variation of RMS and FWHM with martensite content is due to the generation of BN signals from the intra-martensite obstacles.

Growth of the martensite phase occurs by the coalescence of martensite embryos in the steel microstructure^[30-32]. The formation of martensite embryos is believed to occur mostly at the early stages of deformation. It has been reported that when the martensite content exceeds 20%, the growth of the martensite phase is energetically more favourable than the formation of new martensitic embryos^[32]. Therefore, it can be concluded that for the strain values greater than that needed to produce about 40% martensite phase in the steel microstructure at the beginning of the peak height plot of the BN profile (Figure 5), the amount of austenite-martensite interface is reduced with an increase in the strain. When the applied magnetic field is removed from a magnetically-saturated ferromagnetic material, the material remains partially magnetised due to the pinning of DWs behind the obstacles. The reverse applied magnetic field required to free all the DWs from the obstacles (magnetic coercivity) depends on the amount and type (pinning strength) of the obstacles. As concluded before, the austenite-martensite interface is one of the strongest obstacles in the microstructure, whereby the austenite-martensite is the last pinning site from which the DWs will be released. Therefore, one may speculate that the BN signals related to the pinning effect of austenite-martensite interfaces are generated mostly near the magnetic coercivity point (H_c). As mentioned previously, the position of the BN profile peak (PP) represents the magnetic coercivity and hence it can be concluded that the variation of the peak height parameter with martensite content is mostly influenced by the amount of austenite-martensite interface. Consequently, the decreasing slope of the peak height curve (Figure 5) may be attributed to the reduction of these interface areas at high strain values.

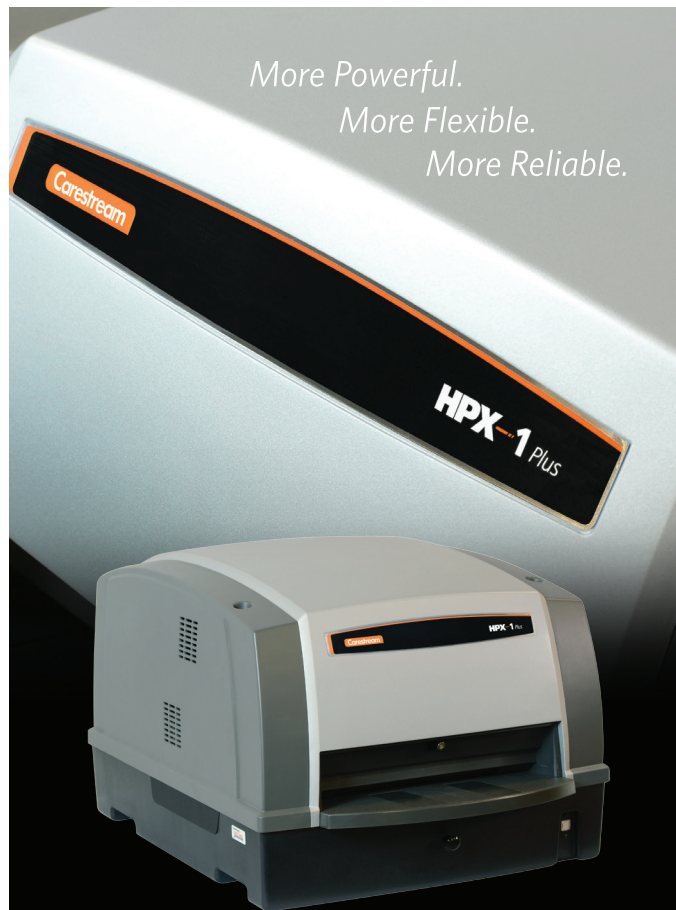
Conclusion

In this study, the capability of the Barkhausen technique in the characterisation of martensitic transformation in an austenitic stainless steel was investigated. It was found that MBN is affected by the amount and size of martensite packets. Increasing martensite content increased the volume fraction of DWs and pinning sites, which, in turn, increased the BN parameters. It was also shown that the coalescence of growing martensite packets in a high-deformation regime provides extensive areas for domain wall motion and this increased the interactions between DWs and pinning sites, resulting in more Barkhausen signals in a wider range of applied fields. However, due to the reduction of austenite-martensite interface areas, the rate of increase in the peak height of the BN profile (Figure 5) decreased.

References

1. W F Smith, *Structure and Properties of Engineering Alloys*, 1993.
2. V Moorthy, S Vaidyanathan, T Jayakumar and B Raj, 'On the influence of tempered microstructures on magnetic Barkhausen emission in ferritic steels', *Philosophical Magazine A*, Vol 77, pp 1499-1514, 1998.
3. C-G Stefanita, 'Barkhausen noise as a magnetic non-destructive testing technique', *From Bulk to Nano: The Many Sides of Magnetism*, pp 19-40, 2008.
4. J Pérez-Benítez, J Espina-Hernández, P Martínez-Ortiz, A Chávez-González and J de la Rosa, 'Analysis of the influence of some magnetising parameters on magnetic Barkhausen noise using a microscopic model', *Journal of Magnetism and Magnetic Materials*, Vol 347, pp 51-60, 2013.
5. D Buttle, C Scruby, J Jakubovics and G Briggs, 'Magnetoacoustic and Barkhausen emission: their dependence on dislocations in iron', *Philosophical Magazine A*, Vol 55, pp 717-734, 1987.
6. F Jarrahi, M Kashefi and E Ahmadzade-Beiraki, 'An investigation into the applicability of the Barkhausen noise technique in the evaluation of machining properties of high carbon steel parts with different degrees of spheroidisation', *Journal of Magnetism and Magnetic Materials*, Vol 385, pp 107-111, 2015.
7. M Vashista and S Paul, 'Correlation between surface integrity of ground medium carbon steel with Barkhausen noise parameters and magnetic hysteresis loop characteristics', *Materials & Design*, Vol 30, pp 1595-1603, 2009.
8. C Gatelier-Rothea, J Chicois, R Fougères and P Fleischmann, 'Characterisation of pure iron and (130 ppm) carbon-iron binary alloy by Barkhausen noise measurements: study of the influence of stress and microstructure', *Acta Materialia*, Vol 46, pp 4873-4882, 1998.
9. S Yamaura, Y Furuya and T Watanabe, 'The effect of grain boundary microstructure on Barkhausen noise in ferromagnetic materials', *Acta Materialia*, Vol 49, pp 3019-3027, 2001.
10. J Rodriguez, J Perez-Benitez, J Capo-Sanchez, L Padovese and R Betancourt-Riera, 'Dependence of Barkhausen jump shape on microstructure in carbon steel', *Revista Mexicana de Física*, Vol 54, pp 127-129, 2008.
11. A Ktena, E Hristoforou, G J Gerhardt, F P Missell, F J Landgraf, D L Rodrigues Jr and M Alberteris-Campos, 'Barkhausen noise as a microstructure characterisation tool', *Physica B: Condensed Matter*, Vol 435, pp 109-112, 2014.
12. D Ng, K Cho, M Wong, S Chan, X-Y Ma and C Lo, 'Study of microstructure, mechanical properties and magnetisation process in low-carbon steel bars by Barkhausen emission', *Materials Science and Engineering: A*, Vol 358, pp 186-198, 2003.
13. K Koo, M Yau, D H Ng and C Lo, 'Characterisation of pearlite grains in plain carbon steel by Barkhausen emission', *Materials Science and Engineering: A*, Vol 351, pp 310-315, 2003.
14. M Kaplan, C Gür and M Erdogan, 'Characterisation of dual-phase steels using magnetic Barkhausen noise technique', *Journal of Nondestructive Evaluation*, Vol 26, pp 79-87, 2007.
15. I Mészáros and J Prohászka, 'Magnetic investigation of the effect of α' -martensite on the properties of austenitic stainless steel', *Journal of Materials Processing Technology*, Vol 161, pp 162-168, 2005.
16. P Haušild, K Kolařík and M Karlík, 'Characterisation of strain-induced martensitic transformation in A301 stainless steel by Barkhausen noise measurement', *Materials & Design*, Vol 44, pp 548-554, 2013.
17. M J Sablik and D C Jiles, 'Coupled magnetoelastic theory of magnetic and magnetostrictive hysteresis', *IEEE Transactions on Magnetics*, Vol 29, pp 2113-2123, 1993.
18. D Jiles, 'Dynamics of domain magnetisation and the Barkhausen effect', *Czechoslovak Journal of Physics*, Vol 50, pp 893-924, 2000.

19. O Stupakov, O Perevertov, V Stoyka and R Wood, 'Correlation between hysteresis and Barkhausen noise parameters of electrical steels', IEEE Transactions on Magnetics, Vol 46, pp 517-520, 2010.
20. O Stupakov, T Uchimoto and T Takagi, 'Magnetic anisotropy of plastically-deformed low-carbon steel', Journal of Physics D: Applied Physics, Vol 43, 195003, 2010.
21. M Blaow, J Evans and B Shaw, 'Magnetic Barkhausen noise: the influence of microstructure and deformation in bending', Acta Materialia, Vol 53, pp 279-287, 2005.
22. B Raj, T Jayakumar, V Moorthy and S Vaidyanathan, 'Characterisation of microstructures, deformation and fatigue damage in different steels using magnetic Barkhausen emission technique', Russian Journal of Nondestructive Testing, Vol 37, pp 789-798, 2001.
23. H Gupta, M Zhang and A Parakka, 'Barkhausen effect in ground steels', Acta Materialia, Vol 45, pp 1917-1921, 1997.
24. C Lo, S Lee, L Kerdus and D Jiles, 'Examination of the relationship between the parameters of the Barkhausen effect model and microstructure of magnetic materials', Journal of Applied Physics, Vol 91, pp 7651-7653, 2002.
25. K Davut and C H Gür, 'Monitoring the microstructural changes during tempering of quenched SAE 5140 steel by magnetic Barkhausen noise', Journal of Nondestructive Evaluation, Vol 26, pp 107-113, 2007.
26. V Moorthy, B Shaw and J Evans, 'Evaluation of tempering-induced changes in the hardness profile of case-carburised EN36 steel using magnetic Barkhausen noise analysis', NDT&E International, Vol 36, pp 43-49, 2003.
27. M Amitava, P De, D Bhattacharya Sr, P Srivastava and D Jiles, 'Ferromagnetic properties of deformation-induced martensite transformation in AISI 304 stainless steel', Metallurgical and Materials Transactions A, Vol 35, pp 599-605, 2004.
28. J Capó-Sánchez, J Pérez-Benitez, L Padovese and C Serna-Giraldo, 'Dependence of the magnetic Barkhausen emission with carbon content in commercial steels', Journal of Materials Science, Vol 39, pp 1367-1370, 2004.
29. S Kobayashi, A Saito, S Takahashi, Y Kamada and H Kikuchi, 'Characterisation of strain-induced martensite phase in austenitic stainless steel using a magnetic minor-loop scaling relation', Applied Physics Letters, Vol 92, pp 182508-182508-3, 2008.
30. K Staudhammer, L Murr and S Hecker, 'Nucleation and evolution of strain-induced martensitic (bcc) embryos and substructure in stainless steel: a transmission electron microscope study', Acta Metallurgica, Vol 31, pp 267-274, 1983.
31. L Murr, K Staudhammer and S Hecker, 'Effects of strain state and strain rate on deformation-induced transformation in 304 stainless steel: Part II. Microstructural study', Metallurgical Transactions A, Vol 13, pp 627-635, 1982.
32. P Hedström, U Lienert, J Almer and M Odén, 'Stepwise transformation behaviour of the strain-induced martensitic transformation in a metastable stainless steel', Scripta Materialia, Vol 56, pp 213-216, 2007.



More Powerful.
More Flexible.
More Reliable.

It's a Plus

The new **HPX-1 Plus CR** system makes NDT radiography simple, accurate, reliable and affordable. It was no surprise that when we introduced the HPX-1 it would raise the bar in the industry. The HPX-1 Plus builds on this foundation with improved optics for better imaging, faster throughput, more efficient erase cycle, better plate transport, and improved viewing software for the best experience in digital imaging.

- HPX-1 Plus has improved optics for optimal imaging.
- Delivers ultra high image quality consistently, with full dynamic range and sensitivity for almost any application.
- Comes fully pre-configured and ready to operate after a few simple connections.
- User-friendly software and intuitive interface minimizes training time; operators will be up and running fast.
- Simplified work-flow improves productivity with enhanced annotation capabilities, automatic file naming and a double file save capability (INDUSTREX and DICONDE).
- Transportable, durable, and designed to perform in the harshest of NDT environments.

YouTube carestream.com

Carestream

© 2015 Carestream, Inc. Rochester, N.Y. 14608